

Battery and supercapacitor for photovoltaic energy storage: a fuzzy logic management

ISSN 1752-1416
Received on 29th May 2016
Revised 8th April 2017
Accepted on 2nd May 2017
E-First on 13th June 2017
doi: 10.1049/iet-rpg.2016.0455
www.ietdl.org

Zineb Cabrane¹ ✉, Mohammed Ouassaid¹, Mohamed Maaroufi¹

¹Department of Electrical Engineering, Mohammadia School of Engineers (EMI), Mohammed V University, Rabat, Morocco

✉ E-mail: zinebcabrane@gmail.com

Abstract: This study presents an approach of the voltage regulation of DC bus for the photovoltaic energy storage by using a combination of batteries and supercapacitors (SCs). The batteries are used to meet the energy requirements for a relatively long duration, whereas the SCs are used to meet the instantaneous power demand. The energy management strategy is developed to manage the power flows between the storage devices by choosing the optimal operating mode, thereby to ensuring the continuous supply of the load by maintaining the state-of-charge (SoC) of SCs (SoC_{SC}) and the SoC of the batteries (SoC_{bat}) at acceptable levels. This energy management strategy is performed by using the fuzzy logic supervisor. The validation results prove the effectiveness of the proposed strategy.

1 Introduction

The photovoltaic (PV) technology has become a favoured form of the renewable energy technology because it is seen as sustainable and clean [1]. The irradiance fluctuation of PV energy may cause excessive variations of the output voltage, power and frequency. However, storage systems have been used to design active generators, which are able to provide an energy reserve in less fluctuating power [2–4]. The most common type of storage of hybrid systems is the chemical storage in the form of a battery.

The modern batteries provide high discharging efficiency and higher energy storage density, but they suffer a relatively low power density. Supercapacitors (SCs) have low internal resistance. Hence, a combination of battery and SC may mitigate the rate capacity effect of high pulsed discharge current [5]. Thus, SCs are, currently, used as short-term power buffers or secondary energy storage devices in renewable energy [6, 7], and power systems [8]. Indeed, this combination is an interesting solution for improving system performance, in terms of the dynamic behaviour of the batteries and their long life [9]. This combination of batteries and SCs was developed successfully in many applications like energy storage system and hybrid power source for vehicle applications [10, 11], energy storage system in autonomous microgrid [12] and hybrid power sources for UPS applications [13].

A fuzzy logic-based algorithm is proposed to solve the energy management problem and the energy distribution between the batteries and SCs. However, the fuzzy logic supervisor (FLS) does not require complex mathematical models as used in classic control. The control by FLS of the energy management system (EMS) is already used in many applications like, EMS for polygeneration microgrids [14], performance evaluation of a grid-independent hybrid renewable energy system [15] and EMS for DC microgrid systems [16]. However, in this work, it used to ensuring the continuous supply of the load by maintaining the state-of-charge (SoC) of the SCs (SoC_{SC}) and the SoC of the batteries (SoC_{bat}) at acceptable levels to avoid the damaging of batteries and SCs.

The remaining of this paper is organised as follows: Section 2 presents the description and modelling of the system under study. The fuzzy logic EMS is addressed in Section 3. To demonstrate the effectiveness of the proposed EMS, some simulation results are presented in Section 4; and finally, in Section 5, conclusions are given.

2 Description and modelling of the system under study

The storage hybrid system of PV energy using the combination of batteries and SCs is shown in Fig. 1.

2.1 Modelling of SC

The equivalent electric circuit of two-branch model is represented in Fig. 2, which is proposed by Zubietta and Bonert [17], Gualous *et al.* [18]. It is formed by two parts, the first, called principal, where the energy is quickly stored, in a few seconds, and corresponds to the first R_1C_1 cells of a distributed-constant model. In the second, called slow, the energy is slowly stored. It supplements the first by the description of the internal redistribution of energy in a few minutes, and corresponds to the latest R_2C_2 [19]. R_f represents the leakage current [20].

The main capacitance C_1 , called differential, depends on the voltage v_1 . It consists of a constant capacity C_0 and a constant parameter C_v and it is given by

$$C_1 = C_0 + C_v \cdot v_1. \quad (1)$$

By neglecting the leakage current, the equivalent circuit of the SC is given by the following equation:

$$U_{SC} = N_{Ssc} v_{SC} = N_{Ssc} \left(v_1 + R_1 \frac{I_{SC}}{N_{Psc}} \right) \quad (2)$$

where U_{SC} and I_{SC} are the SCs pack voltage and current, respectively; v_{sc} is the elementary SC voltage. N_{Psc} and N_{Ssc} are the number of parallel and series branches of the SCs connections, respectively. The voltage v_2 is given by

$$v_2 = \frac{1}{C_2} \int i_2 dt = \frac{1}{C_2} \int \frac{1}{R_2} (v_1 - v_2) dt. \quad (3)$$

The current i_1 in the main capacitor C_1 is expressed in terms of the instantaneous charge Q_1 and C_1 as

$$i_1 = C_1 \frac{dv_1}{dt} = \frac{dQ_1}{dt} = (C_0 + C_v \cdot v_1) \frac{dv_1}{dt} \quad (4)$$

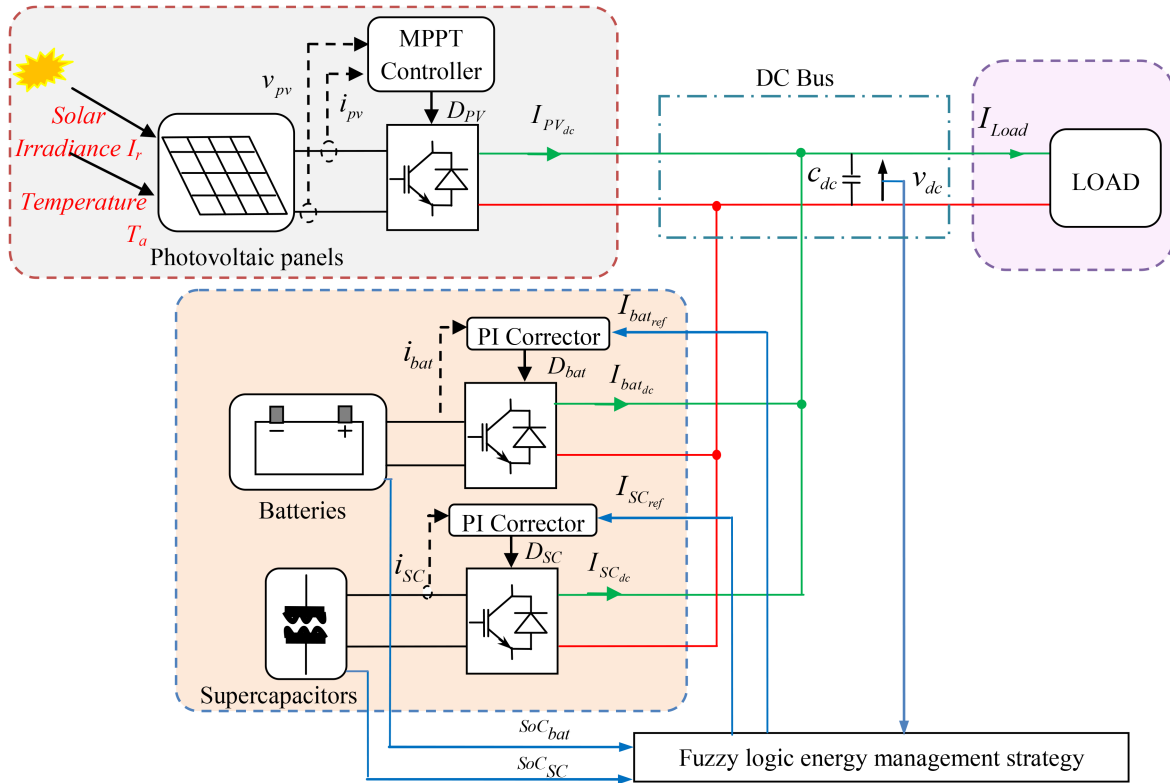


Fig. 1 Configuration of the proposed hybrid system by using a combination of batteries and SCs

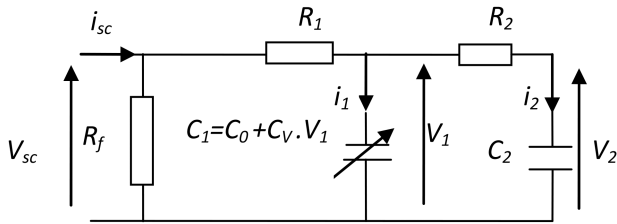


Fig. 2 SC simplified circuit: two-branch model

Table 1 Units for magnetic properties

Parameter	BCAP3000
normal capacitance	3000 V
rated voltage	2.7 V DC
maximum operating voltage	2.85 V DC
maximum ESR, DC initial	0.29 mΩ
operating temperature range (stored uncharged)	-40 to +65°C
storage temperature range (cell case temperature)	-40 to +70°C

Table 2 Parameters of two-branch model of SC

Parameter	Value
R_1	0.8 mΩ
C_0	2170 F
C_v	520 F/V
R_2	1 Ω
C_2	150 F

where the charge Q_1 is given by

$$Q_1 = C_0 \cdot v_1 + \frac{1}{2} C_v \cdot v_1^2 \quad (5)$$

Then the voltage v_1 is defined as follows:

$$v_1 = \frac{-C_0 + \sqrt{C_0^2 + 2C_v Q_1}}{C_v} \quad (6)$$

The parameter specifications of SCs are listed in Table 1. The parameters of the two-branch model are given in Table 2.

2.2 CIEMAT battery model

The battery model used in this work is the CIEMAT model (Centro de investigaciones energéticas medioambientales y tecnológicas: Center for environmental and technological energy research). It is based on the electrical diagram presented in Fig. 3, according to which the battery is described by just two elements: an internal resistance R_i and a voltage source E_b . It has two operation modes: the charge and the discharge.

The following equation represents the relation between the voltage V_{bat} and the current I_{bat} of battery with n_b cells in series:

$$V_{bat} = n_b \cdot E_b + n_b \cdot R_i \cdot I_{bat} \quad (7)$$

The capacity of the battery delivers the quantity of energy C_{bat} that the battery can restore according to the average discharge current I_{bat} . This last is established with respect to discharge current I_{10} corresponding to the rated capacity C_{10} [21]

$$\frac{C_{bat}}{C_{10}} = \frac{1.67}{1 + 0.67 \cdot (I_{bat}/I_{10})^{0.9}} \cdot (1 + 0.005 \cdot \Delta T) \quad (8)$$

3 Fuzzy logic EMS

3.1 Control and management of DC bus

The DC bus voltage is controlled according to the principle described in Fig. 4a. The PI corrector calculates the reference current of DC bus I_{dc_ref} to maintain the bus voltage at the reference voltage $V_{ref} = 400$ V.

The reference currents of batteries and SCs (I_{bat_ref} and I_{sc_ref} , respectively) are delivered by the EMS. These reference currents will allow to keep the DC bus voltage constant regardless of the

load behaviour and the variation of the power extracted from PV generator. The batteries and/or SCs ensure the regulation of the DC bus voltage when a problem occurs on an element such as SoC, power failure, and variation of solar irradiation. At any time, the sum of the reference currents, I_{sc_ref} and I_{bat_ref} , must be equal to I_{dc_ref} .

$$I_{dc_ref} = I_{sc_ref} + I_{bat_ref} \quad (9)$$

The behaviour of the DC bus can be modelled by the following equation:

$$C_{dc} \frac{dv_{dc}}{dt} = i_{sc_dc} + i_{bat_dc} + i_{pv_dc} - i_{Load} \quad (10)$$

where I_{SC_dc} , I_{bat_dc} and I_{pv_dc} , represent the DC currents of SCs, batteries and PV panels, respectively. I_{Load} is the load current. C_{dc} is the central bus capacity that will allow imposing a common DC bus voltage to the load and all other sources. These capacitors filter the power fluctuations from the adopted static converters.

3.2 Energy management system

The reference current of batteries I_{bat_ref} and reference current of SCs I_{sc_ref} are delivered according to the principle shown in Fig. 4b. A low-pass filter is applied to the DC bus current to divert sudden

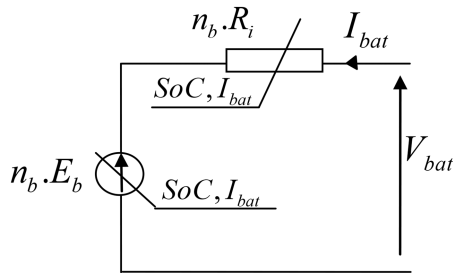


Fig. 3 Equivalent electrical diagram of N_b battery elements in series

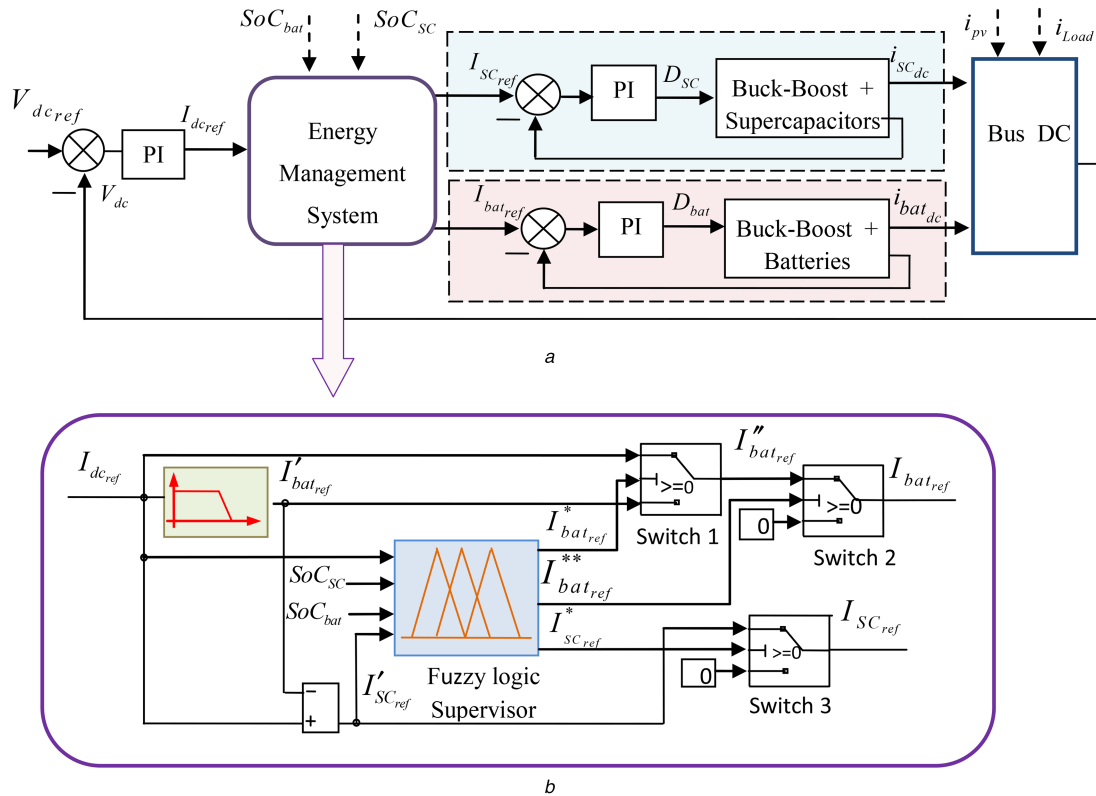


Fig. 4 Control and management of DC bus
(a) Block diagram of the DC bus control, (b) Diagram explaining the EMS

power variation into the SCs. The reference current of the DC bus I_{dc_ref} passes in this filter to construct the batteries current reference I'_{bat_ref} . The SCs current reference I'_{sc_ref} is determined by the difference between I_{dc_ref} and I'_{bat_ref} .

To elaborate the reference currents, the SoC of batteries and the SCs must be taken into account. Three switches are used to select the exact reference current, they are controlled by fuzzy logic in function of $I^*_{bat_ref}$, $I^{**}_{bat_ref}$ and $I^*_{sc_ref}$.

- Switch 1 allows to select between I_{dc_ref} and I'_{bat_ref} .

If I_{dc_ref} is negative and $SoC_{sc} \geq 95\%$ then $I''_{bat_ref} = I_{dc_ref}$, else $I''_{bat_ref} = I'_{bat_ref}$.

If I_{dc_ref} is positive and $SoC_{sc} \leq 25\%$ then $I''_{bat_ref} = I_{dc_ref}$, else $I''_{bat_ref} = I'_{bat_ref}$.

- Switch 2 allows to select between I''_{bat_ref} and 0.

If I_{dc_ref} is negative and $SoC_{bat} \geq 95\%$ then $I_{bat_ref} = 0$, else $I_{bat_ref} = I''_{bat_ref}$.

If I''_{bat_ref} is positive and $SoC_{bat} \leq 25\%$ then $I_{bat_ref} = 0$, else $I_{bat_ref} = I''_{bat_ref}$.

- Switch 3 allows to select between I'_{sc_ref} and 0.

If I'_{sc_ref} is negative and $SoC_{sc} \geq 95\%$ then $I_{sc_ref} = 0$, else $I_{sc_ref} = I'_{sc_ref}$.

If I'_{sc_ref} is positive and $SoC_{sc} \leq 25\%$ then $I_{sc_ref} = 0$, else $I_{sc_ref} = I'_{sc_ref}$.

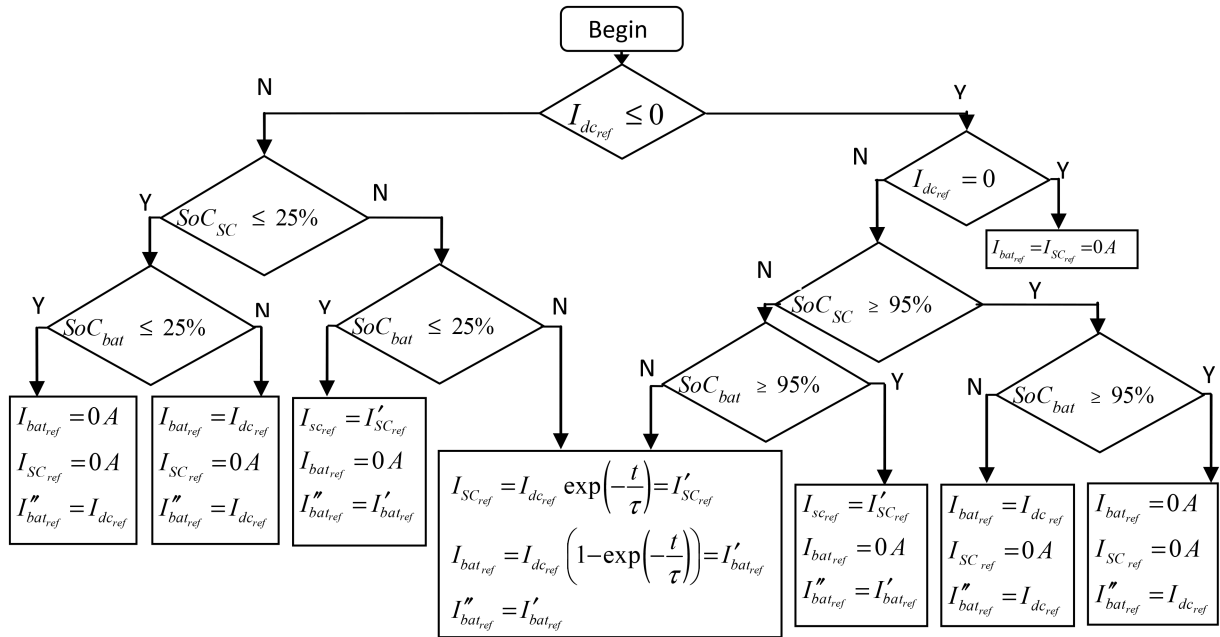


Fig. 5 Flowchart of the Power Management Strategy

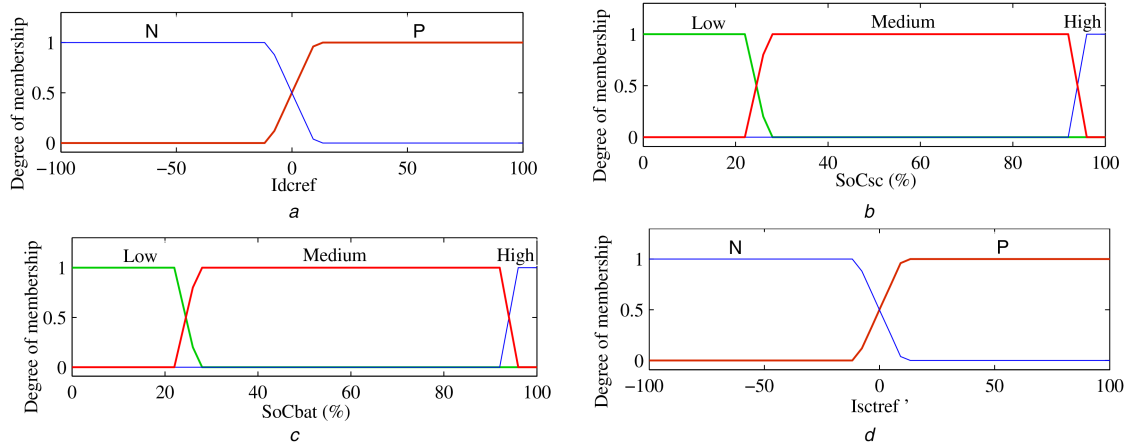


Fig. 6 Block diagram of the proposed inputs FLS-based EMS

(a) Reference current of DC bus I_{dc_ref} , (b) SoC of SCs (SoC_{sc}), (c) SoC of batteries (SoC_{bat}), (d) Reference current of SCs I_{sc_ref}

The flowchart given in Fig. 5 explains the functioning of the EMS by giving the references currents of the batteries and the SCs for different cases of SoC.

- If the reference current of DC bus is negative (when the PV panels give higher than the load power) and the SoC of SCs is $>95\%$ (SCs was saturated) the reference current of SCs must be null. If not the case, SCs begin to charge.
- If the reference current of DC bus is positive (when the PV panels fail to give the desired power) and the SoC of SCs is $<25\%$ the reference current of SCs must be null. If the SoC_{sc} is $>25\%$ SCs begin to discharge.
- The reference current of DC bus is null when the PV panels produce the power needed by the load.

3.3 FLS strategy

The objective behind using fuzzy logic in this study is to manage the overall system power flow while maintaining the SoC of batteries and the SoC of the SCs at their admissible intervals of their SoC. The FLS utilised in this study includes four inputs and three outputs as shown in Figs. 6 and 7.

The inputs of the FLS are the reference current of DC bus I_{dc_ref} , the SoC of batteries SoC_{bat} , the SoC of SCs (SoC_{sc}) and the

reference current of SCs. The outputs are the reference current of batteries $I_{bat_ref}^*$ for the command of the switch 1, the reference current of batteries $I_{bat_ref}^{**}$ for the command of the switch 2 and the reference current of SCs $I_{sc_ref}^*$ for the command of the switch 3. Using the data available from these four inputs, the FLC determines the command of the three switches used for the regulation of the DC bus according to the principle described in the flowchart.

3.3.1 Determination of the membership functions: The aim of the proposed methodology is to define membership functions for the input and output variables for the FLS. The input membership functions are used as transitions between the different operating modes. They are shown in Figs. 6 and 7.

The membership functions of the storage levels (Figs. 6a and d) are based on two levels to accommodate the needs of the proposed strategy, N stands for negative and P stands for positive where they represent the sign of the reference current I_{dc_ref} and I_{sc_ref} , with N and P represent the charge and discharge of SCs and batteries, respectively. The reference currents I'_{sc_ref} and I_{dc_ref} are considered between 100 and -100 A.

Figs. 6b and c represent the membership of SoC of the batteries (SoC_{bat}) and SoC of the SCs (SoC_{sc}). In the same way, three levels are defined:

- The low level representing the SoC is $<25\%$ (between 0 and 25%).
- The medium level representing the SoC is between 25 and 95%.
- The high level representing the SoC is $>95\%$ (between 95 and 100%).

The output membership functions are shown in Figs. 7a–c, the command of switch 1 for the reference current of batteries $I_{bat,ref}^*$, the command of switch 2 for the reference current of batteries $I_{bat,ref}^{**}$ and the command of switch 3 for the reference current of SCs $I_{sc,ref}^*$. These functions are based on two levels, N stands for negative and P stands for positive where they represent the sign of

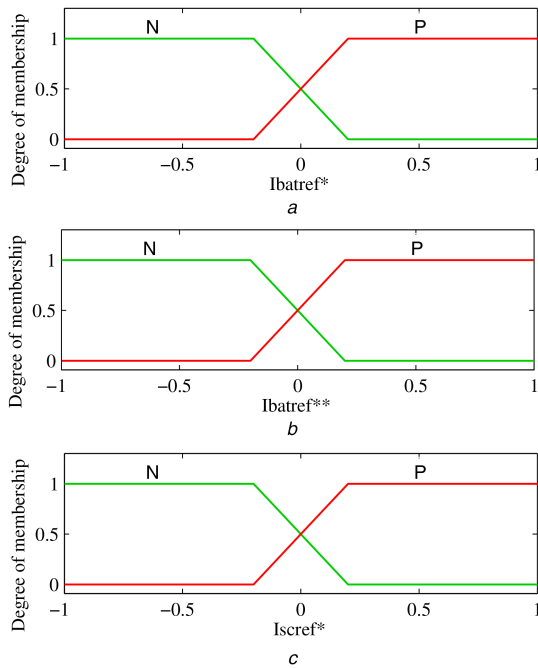


Fig. 7 Block diagram of the proposed outputs FLS-based EMS
(a) Reference current of batteries $I_{bat,ref}^*$, (b) Reference current of batteries $I_{bat,ref}^{**}$, (c) Reference current of SCs $I_{sc,ref}^*$

Table 3 $I_{bat,ref}^*$ rules

	SoC _{bat}		
	Low	Medium	High
$I_{dc,ref}$	N	P	N
	P	N	P

Table 4 $I_{bat,ref}^{**}$ rules

	SoC _{sc}		
	Low	Medium	High
$I_{dc,ref}$	N	P	N
	P	N	P

Table 5 $I_{sc,ref}^*$ rules

	SoC _{sc}		
	Low	Medium	High
$I_{sc,ref}$	N	P	N
	P	N	P

the command of the switches. The output membership functions are estimated between 1 and -1.

3.3.2 Fuzzy supervisor rules: The fuzzy supervisor rules used for the EMS are obtained from the analysis of the system behaviour. In their formulation, it must be considered that using different control laws depending on the operating conditions can improve the performances of the EMS. The control rules that associate the fuzzy input to the fuzzy output is made up of three parts which are as follows:

- Table 3 represents the fuzzy rules used between SoC_{bat} and $I_{dc,ref}$ to obtain the command $I_{bat,ref}^*$ of switch 1. The fuzzy rules are divided into six parts.
- The fuzzy rules that are used between SoC_{sc} and $I_{dc,ref}$ to obtain the command $I_{bat,ref}^{**}$ of switch 4 are shown in Table 4.
- Table 5 represents the fuzzy rules used between SoC_{sc} and $I_{sc,ref}^*$, it's used to obtain the command $I_{sc,ref}^*$ of switch 3.

4 Simulation results and validation

The studied system has been implemented with different operating conditions in the MATLAB/SIMULINK environment. To ensure the continuous supply of the load and to do not damage the batteries and the SCs we must maintain the SoC of the SCs (SoC_{sc}) and the SoC of the batteries (SoC_{bat}) at acceptable levels. The low rate of charge of batteries and SCs are 25% and the high rate of charge of batteries and SCs are 95%.

All simulation tests are executed by a time constant of the low-pass filter at $\tau = 6$ s. The structure of simulation setup diagram is represented in Fig. 8.

The first simulation test, as shown in Fig. 9, was carried out with a constant solar irradiance of 1000 W/m² and with different values of load currents [120, 200, 120, 90 A]. The initial SoC of batteries is considered at 50% and the initial SoC of SCs is considered at 29.5%. This simulation test is executed with a classic control in MATLAB/SIMULINK and without FLS.

Fig. 9a represents the PV current I_{pv} and the load current I_{load} . The variation of the batteries current and the SCs current are shown in Fig. 9b and c, respectively. The SoC of SCs (SoC_{sc}) is represented in Fig. 9d. In the case where SCs are fully discharged, when the SoC_{sc} reaches 25%, SCs must stop to discharge and the batteries give all the currents demanded by the load, but is not the case, SCs continues to give current fluctuations (between 15 and 25 s) and the batteries also.

In the following results, we propose to use the management of energy distribution by the FLS.

The second simulation test is executed with the same conditions of the first one (solar irradiance, load current, the initial SoC of SCs and initial SoC of battery).

Fig. 10a represents the batteries and the SCs currents, the batteries react more slowly to the needs while the SCs provide the transient currents. Fig. 10b shows the variation of the PV current I_{pv} and the load current I_{load} . The SoC of SCs (SoC_{sc}) is represented in Fig. 10d. The DC bus voltage is shown in Fig. 10c, it's considered constant 400 V with small variations. In the case where SCs are fully discharged, the SoC_{sc} reaches 25%, SCs stop to discharge and the batteries give all the currents demanded by the load.

By comparing the first and the second simulation test, we notice that the energy management strategy by using FLS gives excellent results. However, SCs stops to discharge and the batteries give all the currents demanded by the load.

The third simulation test was performed with a constant solar irradiance of 1000 W/m² and with different values of load currents [120, 90, 135, 80 A] as shown in Fig. 11.

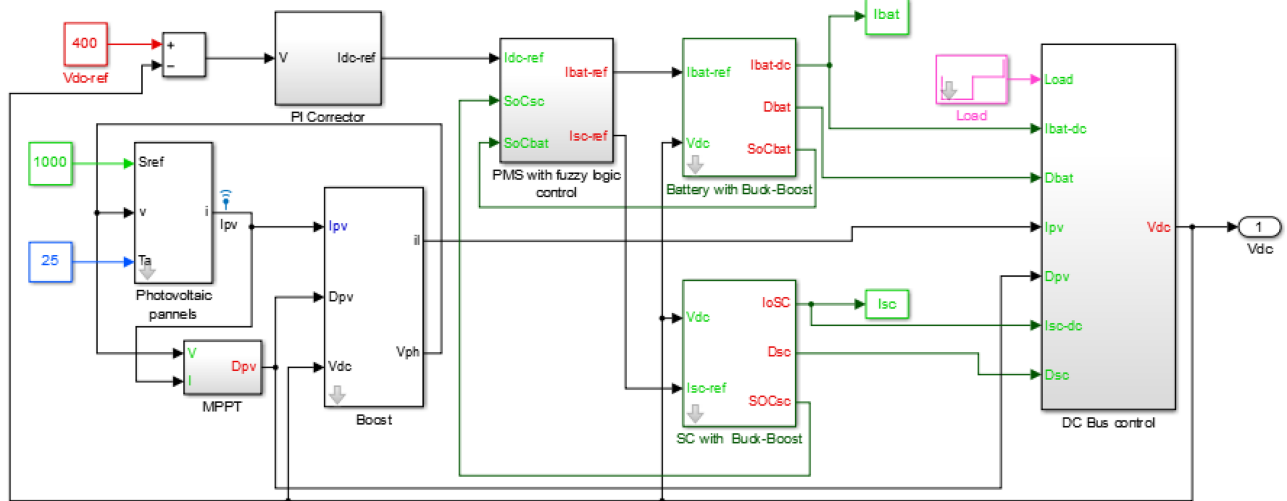
The initial SoC_{bat} is considered at 50% and the initial SoC_{sc} is considered at 94%. The PV current I_{pv} and load current I_{Load} are

represented in Fig. 11a where the load current is considered constant at 120 A and the PV current is considered variable. Fig. 11b illustrates the batteries current and the SCs current, the batteries react more slowly to the needs while the SCs provide the transient currents. The DC bus voltage is shown in Fig. 11c. The SoC_{sc} is represented in Fig. 11d.

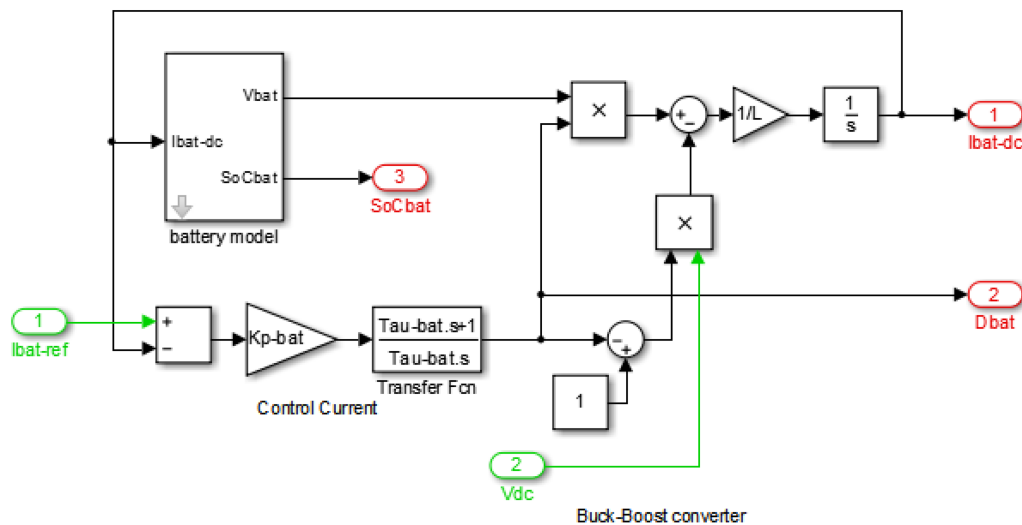
We notice that in the case where SCs are fully charged, the SoC_{sc} reaches 95%, SCs stop to charge. Hence, the batteries absorb all the difference currents between the load and the PV current.

We demonstrate during simulations of PV energy storage by using a combination of batteries–SCs that the SCs reply directly to

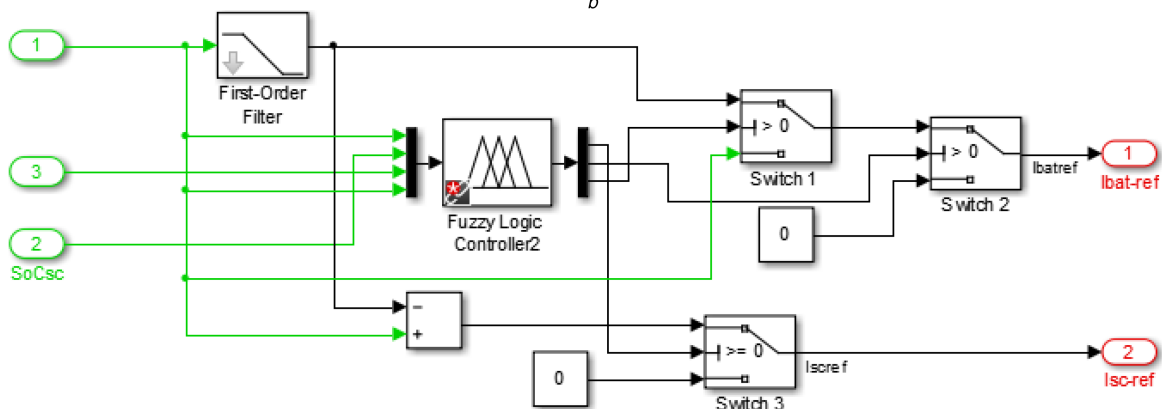
the need of the load. The batteries react more slowly to the needs while SCs provide the transient currents as demanded by the $I_{bat,ref}$ and $I_{SC,ref}$ due to the use of the low-pass filter. The SC current compensates the difference between the batteries current and load current. Consequently, the proposed of the EMS supervisor, based on fuzzy logic, represents a reliable and efficient energy management. However, the simulation results prove the effectiveness of the proposed strategy by keeping a DC bus voltage at 400 V and allow to maintain the SoC_{sc} and SoC_{bat} at acceptable levels.



a



b



c

Fig. 8 Continued

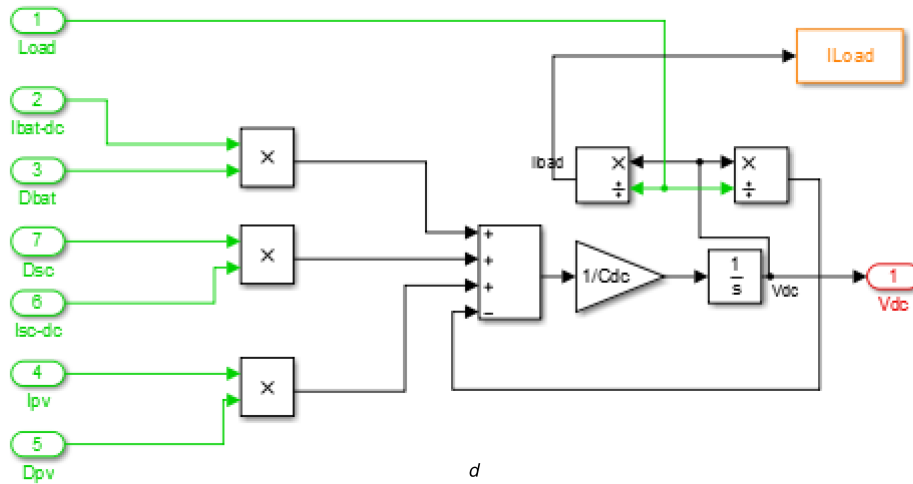


Fig. 8 Structure of simulation setup diagram in MATLAB/SIMULINK
 (a) General program, (b) Control of batteries, (c) PMS with fuzzy logic control, (d) DC bus control

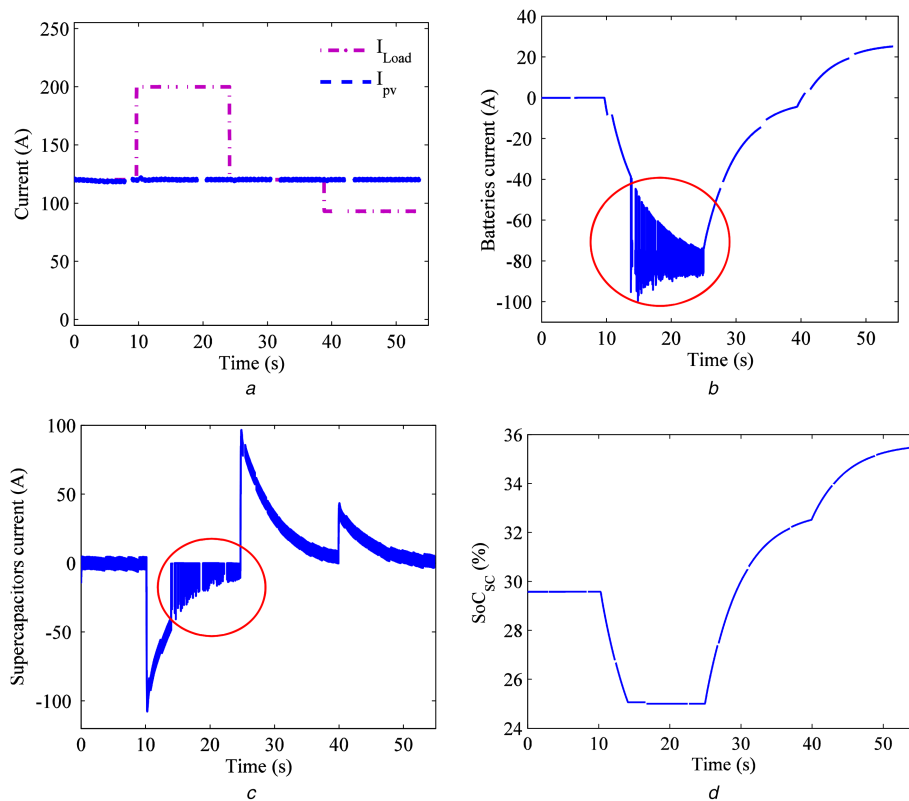


Fig. 9 Simulation result with different load values, with a SoC_{sc} under 25% and a classic control in MATLAB/SIMULINK
 (a) PV current I_{pv} and load current I_{Load} . (b) Batteries current I_{bat} . (c) SCs current I_{sc} . (d) SoC of SCs (SoC_{sc})

5 Conclusion

In this paper, a management strategy of PV energy storage, using battery–SC combination, has been developed.

To this end, a control technique and regulation of the DC bus voltage was proposed in order to deal with the variation of the load and the fluctuation of the solar irradiation. The diagram of EMS used was based on FLS to maintain the batteries and SCs at admissible intervals of their SoC. Simulation results with different values of load and different values of solar irradiation prove the effectiveness of the proposed strategy energy management.

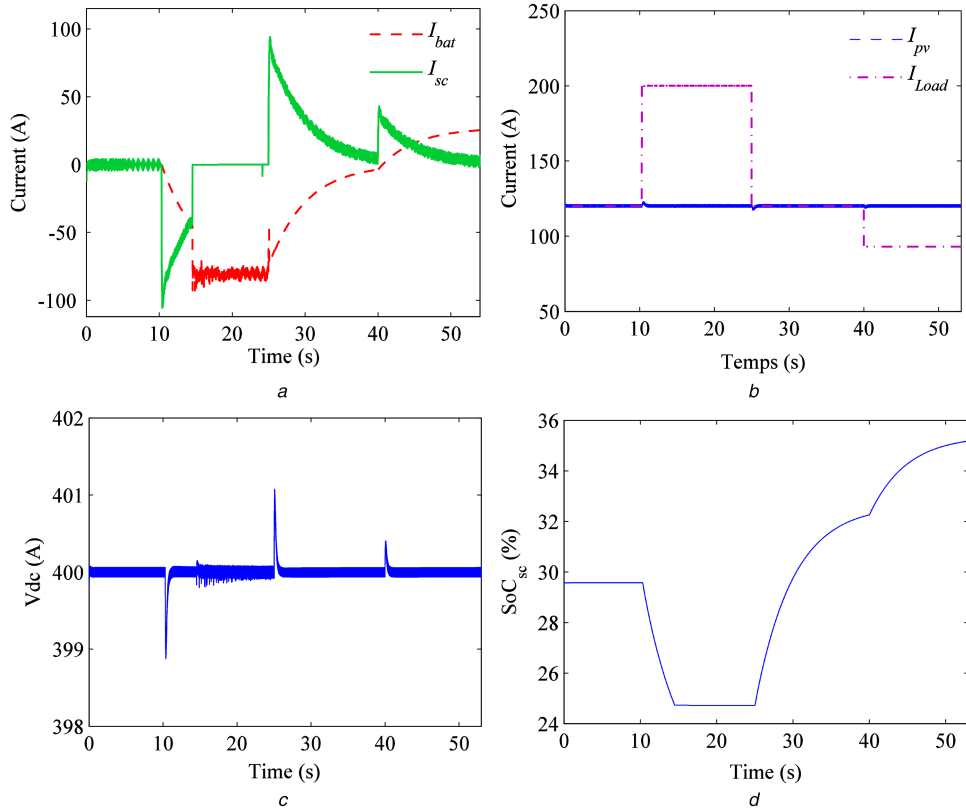


Fig. 10 Simulation result with different load values with a SoC_{sc} under 25% by FLS

(a) Batteries current I_{bat} and SCs current I_{sc} , (b) PV current I_{pv} and load current I_{Load} , (c) DC bus voltage, (d) SoC of SCs (SoC_{sc})

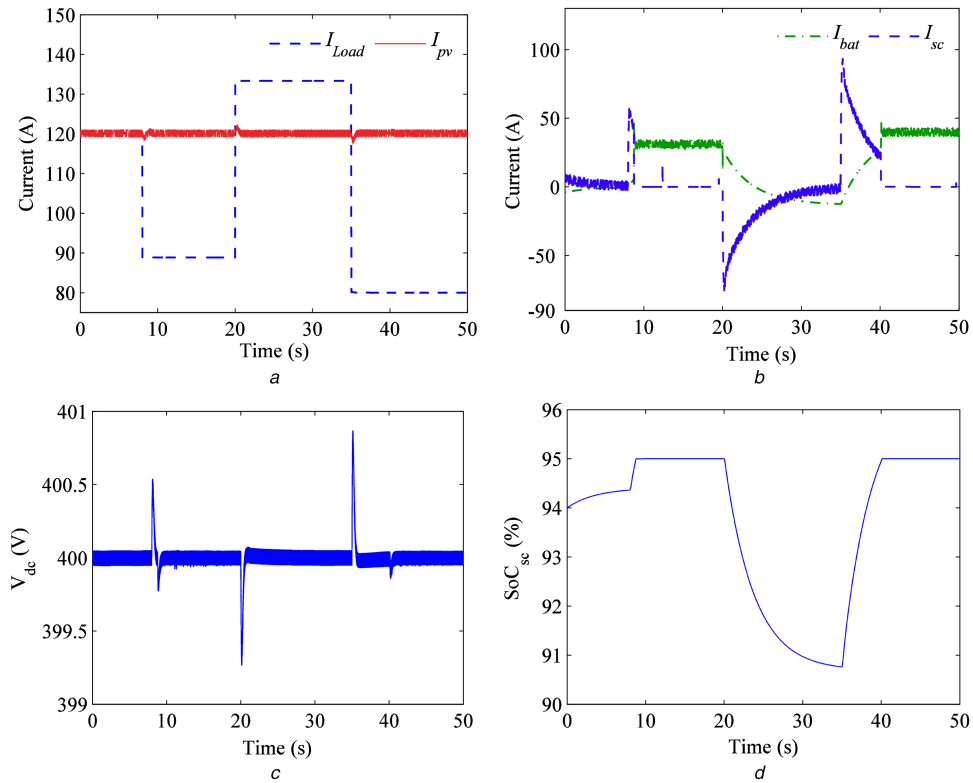


Fig. 11 Simulation result with different load values with a $SoC_{sc} > 95\%$

(a) PV current I_{pv} and load current I_{Load} , (b) Batteries current I_{bat} and SCs current I_{sc} , (c) DC bus voltage, (d) SoC of SCs (SoC_{sc})

6 References

- [1] Wang, Y., Lin, X., Kim, Y., *et al.*: 'Architecture and control algorithms for combating partial shading in photovoltaic systems', *IEEE Trans. Comput.-Aided Des. Integr. Circuits Syst.*, 2014, **6**, (33), pp. 917–930
- [2] Kanchev, H., Lu, D., Colas, F., *et al.*: 'Energy management and operational planning of a microgrid with a PV-based active generator for smart grid applications', *IEEE Trans. Ind. Electron.*, 2011, **10**, (58), pp. 4583–4592
- [3] Fakham, H., Lu, D., Francois, B.: 'Power control design of a battery charger in a hybrid active PV generator for load following applications', *IEEE Trans. Ind. Electron.*, 2011, **1**, (58), pp. 85–94
- [4] Wang, Y., Lin, X., Pedram, M.: 'Adaptive control for energy storage systems in households with photovoltaic modules', *IEEE Trans. Smart Grid*, 2014, **2**, (5), pp. 992–1001
- [5] Shin, D., Kim, Y., Wang, Y., *et al.*: 'Constant-current regulator-based battery-supercapacitor hybrid architecture for high-rate pulsed load applications', *J. Power Sources*, 2012, **205**, pp. 516–524
- [6] Jiang, W., Zhang, L., Zhao, H., *et al.*: 'Research on power sharing strategy of hybrid energy storage system in photovoltaic power station based on multi-objective optimisation', *IET Renew. Power Gener.*, 2016, **5**, (10), pp. 575–583
- [7] Uzunoglu, M., Alam, M.S.: 'Dynamic modeling, design, and simulation of a combined PEM fuel cell and ultracapacitor system for stand-alone residential applications', *IEEE Trans. Energy Convers.*, 2006, **3**, (21), pp. 767–775
- [8] Roberts, B.P., Sandberg, C.: 'The role of energy storage in development of smart grids', *Proc. IEEE*, 2011, **6**, (99), pp. 1139–1144
- [9] Khaligh, A., Zhihao, L.: 'Battery, ultracapacitor, fuel cell, and hybrid energy storage systems for electric, hybrid electric, fuel cell, and plugin hybrid electric vehicles: state-of-the-art', *IEEE Trans. Veh. Technol.*, 2010, **6**, (59), pp. 2806–2814
- [10] Song, Z., Li, J., Han, X., *et al.*: 'Multi-objective optimization of a semi-active battery/supercapacitor energy storage system for electric vehicles', *Appl. Energy*, 2014, **135**, pp. 212–224
- [11] Thounthong, P., Raël, S., Davat, B.: 'Energy management of fuel cell/battery/supercapacitor hybrid power source for vehicle applications', *J. Power Sources*, 2009, **193**, pp. 376–385
- [12] Jia, H., Mu, Y., Qi, Y.: 'A statistical model to determine the capacity of battery–supercapacitor hybrid energy storage system in autonomous microgrid', *Electr. Power Energy Syst.*, 2014, **54**, pp. 516–524
- [13] Zhan, Y., Guo, Y., Zhu, J., *et al.*: 'Power and energy management of grid/PEMFC/battery/supercapacitor hybrid power sources for UPS applications', *Electr. Power Energy Syst.*, 2015, **67**, pp. 598–612
- [14] Kyriakarakos, G., Dounis, A.I., Arvanitis, K.G., *et al.*: 'A fuzzy logic energy management system for polygeneration microgrids', *Renew. Energy*, 2012, **41**, pp. 315–327
- [15] Erdinc, O., Uzunoglu, M.: 'The importance of detailed data utilization on the performance evaluation of a grid-independent hybrid renewable energy system', *Int. J. Hydrog. Energy*, 2011, **36**, pp. 12664–12677
- [16] Chen, Y., Wu, Y., Song, C., *et al.*: 'Design and implementation of energy management system with fuzzy control for DC microgrid systems', *IEEE Trans. Power Electron.*, 2013, **4**, (28), pp. 1563–1570
- [17] Zubieta, L., Bonert, R.: 'Characterization of double-layer capacitors for power electronics applications', *IEEE Trans. Ind. Appl.*, 2000, **1**, (36), pp. 199–205
- [18] Gualous, H., Bouquain, D., Bertbon, A., *et al.*: 'Experimental study of supercapacitor serial resistance and capacitance variations with temperature', *J. Power Sources*, 2003, **123**, pp. 86–93
- [19] Belhachemi, F., Rael, S., Davat, B.: 'A physical based model of power electric double-layer supercapacitors'. IEEE Industrial Application Conf., 2000, no. 5, pp. 3069–3076
- [20] Lahyani, A., Venet, P., Guermazi, A., *et al.*: 'Battery/supercapacitors combination in uninterruptible power supply (UPS)', *IEEE Trans. Power Electron.*, 2013, **4**, (28), pp. 0885–8993
- [21] Achaibou, N., Haddadi, M., Malek, A.: 'Modeling of lead acid batteries in PV systems', *Energy Procedia*, 2012, **18**, pp. 538–544